

Singlet Fission in Lycopene H-Aggregates

William Barford*

*Department of Chemistry, Physical and Theoretical Chemistry Laboratory,
University of Oxford, Oxford, OX1 3QZ, United Kingdom*

E-mail: william.barford@chem.ox.ac.uk

Abstract

A theory of singlet fission (SF) in carotenoid dimers is applied to explain the SF in lycopene H-aggregates observed after high energy photoexcitation. The explanation proposed here is that a high energy, delocalized bright ($^1B_u^-$) state first relaxes and localizes onto a single lycopene monomer. The high-energy intramonomer state then undergoes internal conversion to the $^1B_u^-$ state. Once populated, the $^1B_u^-$ state allows exothermic bimolecular singlet fission, while its internal conversion to the $^2^1A_g^-$ state is symmetry forbidden. The simulation of SF predicts that the intramonomer triplet-pair state undergoes complete population transfer to the intermonomer singlet triplet-pair state within 100 ps. ZFS interactions then begin to partially populate the intermonomer quintet triplet-pair state up to ca. 2 ns, after which hyperfine interactions thermally equilibrate the triplet-pair states, thus forming free, single triplets within ca. 0.1 μ s.

Singlet fission in polyacenes is a photophysical process that has been studied for over 50 years, with numerous reviews covering the topic.¹⁻⁵ In that time a consensus seems to have emerged as to the initial mechanisms of this process: namely, that after photoexcitation into the bright singlet state of a single chromophore, this state undergoes bimolecular fission into two triplets via a two-step electron-hole transfer.^{2,6,7} Research into singlet fission in polyacenes is now generally focussed on how to improve the triplet yield in pursuit of technological applications, which requires a full understanding of the fate of the triplet-pair.⁴

In contrast, an understanding of singlet fission in oligoenes,^{8,9} polyenes¹⁰⁻¹² and carotenoids¹³⁻¹⁹ is still in its infancy.^{3,20-23} A consensus does not exist on the fundamental question as to whether singlet fission in these systems proceeds in the same manner as for polyacenes,¹⁶ or whether an intermediate intramolecular correlated triplet-pair state is involved in the process.^{24,25}

The possibility that an intermediate intramolecular triplet-pair state is involved in singlet fission is suggested by the well-known fact that the lowest excited singlet states of polyenes are indeed a superposition of correlated triplet-pairs²⁶⁻²⁸ and charge-transfer exciton states²⁸ that are populated within 50 fs of photoexcitation of the 'bright' Frenkel exciton state. However, since the triplets in the *lowest* energy 'dark' state (i.e., the 2^1A_g state) are strongly bound,^{28,29} a theory that involves a 'dark' state in singlet fission also has to explain why it is an exothermic process with a high yield of free triplets.

In this letter we develop a theoretical model of singlet fission that qualitatively explains a recent experimental investigation of singlet fission in lycopene H-aggregates by Kundu and Dasgupta.¹⁸ In their work, Kundu and Dasgupta observed that singlet fission only occurs when the lycopene H-aggregates are excited at ca. 350 nm (ca. 3.5 eV), i.e., directly into the blue-shifted H-aggregate absorption band. In contrast, excitation in the 400 - 500 nm (2.5 - 3.1 eV) range, which corresponds to the monomer absorption band, does not cause singlet fission (see Figure 1 of ref¹⁸). This observation indicates that excess energy is needed to facilitate singlet fission.

Another important observation of Kundu and Dasgupta is that the transient excited state absorption reveals an intermediate state generated after photoexcitation that has the characteristic

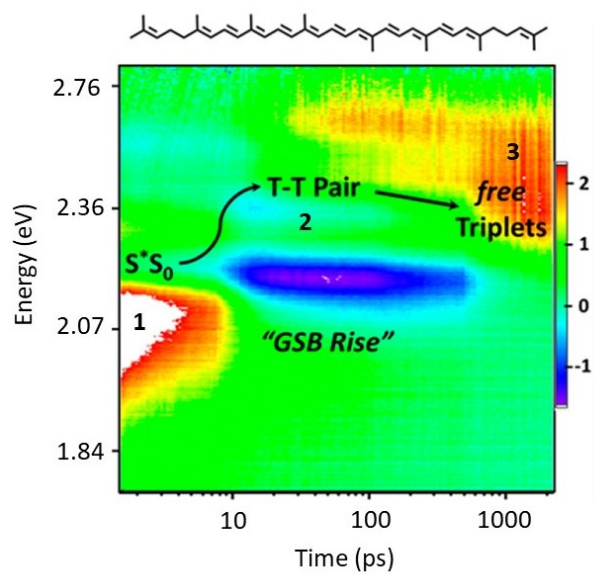


Figure 1: The measured¹⁸ transient excited-state-absorption of a lycopene H-aggregate following photoexcitation at 3.15 eV. See Fig. 4 and the text following it for an explanation of the photo-physics. Reproduced and modified with permission from Kundu, A., Dasgupta, J., *J. Phys. Chem. Lett.* 2021, 12, 1468.

signature of a member of the ‘ $2A_g$ ’ family of strongly correlated states. As has been shown by Barford and co-workers,^{22,29} it is the charge-transfer exciton component of these correlated states that absorbs at ca. 2.1 eV, at an energy red-shifted by 0.3 eV from the free-triplet signal. This is precisely what is observed by Kundu and Dasgupta, as shown in Fig. 1. Importantly, the modeling of their transient data led Kundu and Dasgupta to associate this feature as a higher-energy, intermediate triplet-pair state, i.e., $1^1B_u^-$ or S_1^* . This is significant, because as shown below, unlike for the $2^1A_g^-$ state, exothermic intermonomer singlet fission is possible from the $1^1B_u^-$ state.^{29,30}

Using time-dependent DMRG calculations of the Hubbard-UV-Peierls model, Manawadu and co-workers^{30,31} simulated the internal conversion from the bright state in the related carotenoid, zeaxanthin. Zeaxanthin has 18 conjugated C-atoms (i.e., 9 double bonds) and like lycopene (shown in Fig. 1) possesses C_2 symmetry. According to the simulation, excitation into the bright $1^1B_u^+$ state is followed within 10 fs by adiabatic internal conversion to the $1^1B_u^-$ state via an avoided crossing of S_2 and S_3 . However, as a consequence of C_2 symmetry, to zeroth-order in the Born-Oppenheimer approximation, subsequent internal conversion to the $2^1A_g^-$ state (S_1) is symmetry forbidden.

Here, we propose a somewhat different mechanism of internal conversion for a lycopene monomer within a H-aggregate. In particular, optical excitation into the blue-shifted absorption band of the H-aggregate excites a high-energy $^1B_u^+$ state that is delocalized over a number of monomers. As a consequence of electron-nuclear coupling and intermolecular interactions, this state rapidly relaxes and localizes onto a single monomer. It then undergoes nonadiabatic internal conversion to an intramonomer $^1B_u^-$ state. (This process is similar to the nonadiabatic relaxation and localization of high energy excited states of a conjugated polymer onto a single chromophore described in ref.³²) The timescale for internal conversion is determined by how fast energy is dissipated, but it is expected to ca. 100 fs.³² Bimolecular exothermic singlet fission then follows, as the relaxed energy of the $^1B_u^-$ state lies ca. 0.4 eV above the relaxed energies of a pair of triplets on separate monomers. Importantly, because of symmetry constraints, subsequent internal conversion from the $^1B_u^-$ state to the $^2^1A_g^-$ state is a slow Herzberg-Teller-allowed process. Conversely, bimolecular interstate conversion from $^1B_u^-$ to $T_1^i \otimes T_1^j$ (where i and j label the monomers) is not symmetry forbidden provided that the monomers in the H-aggregate are not perfectly aligned. This scheme is shown schematically in Fig. 2.

Following the generation of intermonomer triplets, the triplets diffuse into the aggregate, thus preventing intermonomer recombination into the $^2^1A_g^-$ state. Alternatively, as shown in ref.²² additional torsional relaxation can stabilize the free triplets relative to the $^2^1A_g^-$ state, thus making recombination an endothermic process.

Before discussing our simulations of the singlet fission process, we first address the question as to why excitation into the monomer absorption band does not cause singlet fission in lycopene.¹⁸ To answer this question we turn to the energy levels of monomeric lycopene obtained via DMRG calculations³³ of the Hubbard-UV-Peierls model for a monomer of 22 carbon sites. (Details of this model and its parametrization are given in the SI.)

In both the theoretical and experimental literature there is uncertainty about the exact relative energies of the vertical $^1B_u^+$, $^2^1A_g^-$, and $^1B_u^-$ states in carotenoids. These energies are highly sensitive to monomer-length and dielectric screening. Some high-level ab initio calculations^{34,35}

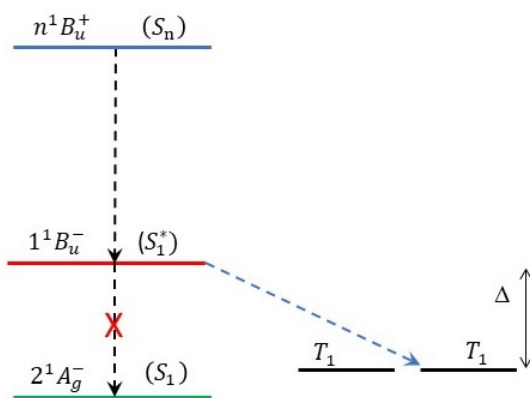


Figure 2: A schematic energy level diagram for some states of lycopene (the approximate adiabatic state labels are in parentheses). The singlet states are on the left, while on the right is the energy level of two triplet states on separate monomers. Here we assume that there is localization and internal conversion from a high-energy, delocalized bright state (here labeled S_n) into the intramonomer $1^1B_u^-$ state, which then undergoes exothermic intermonomer singlet fission. To zeroth-order in the Born-Oppenheimer approximation, interconversion from the $1^1B_u^-$ state to the $2^1A_g^-$ state is symmetry forbidden. Bimolecular interstate conversion from $1^1B_u^-$ to $T_1^i \otimes T_1^j$ (where i and j label the monomers) is not symmetry forbidden provided that the monomers in the H-aggregate are not perfectly aligned. Δ is the exothermic driving energy from the $1^1B_u^-$ state.

predict that the vertical $2^1A_g^-$ state lies above the vertical $1^1B_u^+$ state. In this case, excitation into the $1^1B_u^+$ state causes a $2^1A_g^- - 1^1B_u^+$ level crossing. Alternatively, some semiempirically parametrized Hamiltonians³⁰ predict that the vertical $2^1A_g^-$ state lies below the vertical $1^1B_u^+$ state, while the vertical $1^1B_u^-$ lies above it. In this case, excitation into $1^1B_u^+$ causes a $1^1B_u^- - 1^1B_u^+$ level crossing. In previous work, we have modeled both situations by modifying the parameters of the Hubbard-UV model.²² The energy levels for lycopene for the two different semiempirical parameter sets are shown in Fig. 3. Panel (a) illustrates the $2^1A_g^- - 1^1B_u^+$ level crossing while panel (b) illustrates the $1^1B_u^- - 1^1B_u^+$ level crossing.

The absence of singlet-fission in lycopene under low-energy excitation is explained if a $2^1A_g^- - 1^1B_u^+$ level crossing occurs (i.e., case (a)). In this case, the $2^1A_g^-$ state is populated from the $1^1B_u^+$ state via Herzberg-Teller coupling, and from which singlet fission is endothermic. However, high-energy excitation of a H-aggregate implies that a bright $1^1B_u^+$ state lies higher in energy than the $1^1B_u^-$ state, allowing the latter to be populated (as discussed above and shown schematically in Fig.

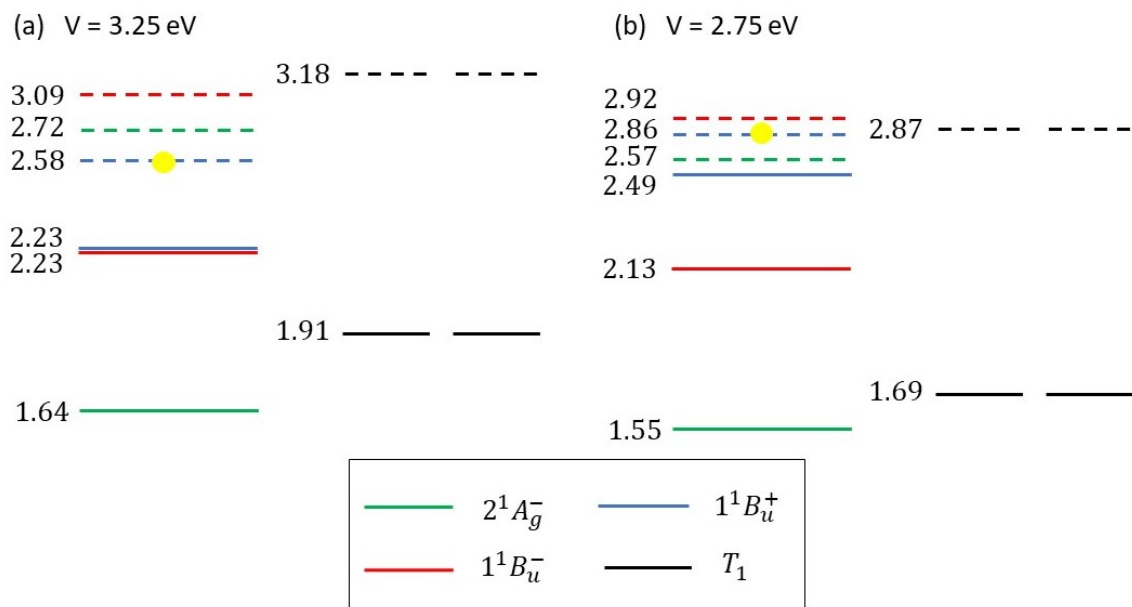


Figure 3: Vertical (dashed lines) and relaxed (solid lines) excitation energies (in eV) of the low-energy states of monomeric lycopene. These are obtained by DMRG calculations of the Hubbard-UV-Peierls model, as explained in the SI. The *intramonomer* singlet states are on the left of each panel, while on the right of each panel is the energy level of two triplet states on separate monomers. In both cases intermonomer singlet fission is (potentially) exothermic (endothermic) from the $1^1B_u^-$ ($2^1A_g^-$) state. The yellow circle indicates the initially excited monomeric ‘bright’ state. (a) The nearest-neighbor Coulomb repulsion, $V = 3.25$ eV; in this case there is level crossing between the $1^1B_u^+$ and $2^1A_g^-$ states. (b) $V = 2.75$ eV; in this case there is level crossing between the $1^1B_u^+$ and $1^1B_u^-$ states.

2). As already mentioned, once populated the $1^1B_u^-$ state can undergo exothermic intermonomer singlet fission, or slow (Herzberg-Teller allowed) internal conversion to the $2^1A_g^-$ state.

Assuming, now, that a singlet triplet-pair state has been formed (i.e., $1^1B_u^-$), we turn to discuss the singlet fission process. To simulate this process, we adopt the theory introduced by Barford and Chambers to explain singlet fission in carotenoid dimers.²³ The key assumptions of this theory are that singlet fission in carotenoid dimers occurs via one of the highly correlated dark states and that these dark states may be regarded as composed entirely of a singlet triplet-pair. Therefore, the charge-transfer exciton component of the dark state²⁸ is assumed to be virtual component that acts to mediate the large intramonomer nearest neighbor triplet exchange interaction,^{23,36}

$$\hat{H}_{\text{exchange}} = J\hat{\mathbf{S}}_i \cdot \hat{\mathbf{S}}_{i+1}. \quad (1)$$

Here, $\hat{\mathbf{S}}$ is the spin-1 (triplet) operator and J is the *inter*triplet exchange interaction. Thus, the intramonomer singlet and triplet triplet-pairs experience a nearest-neighbor attraction, $+2J$ and $+J$, respectively, while the quintet triplet-pair experiences a nearest-neighbor repulsion $-J$. As shown in ref,²³ a value of $J = 1.23$ eV reproduces the intramonomer $1^5A_g^- - 2^1A_g^-$ energy gap of 0.4 eV.²⁹

Triplets hop between ethylene dimers on the same lycopene monomer with a transfer integral, $t_{\text{intra}} = 0.88$ eV,²³ which results in a band of bound singlet triplet-pair states (the ‘ $2A_g$ ’ family of states²⁹), i.e., $2^1A_g^-$, $1^1B_u^-$, $3^1A_g^-$, \dots . For convenience, these strongly interacting, intramonomer states are labeled $^1|TT\rangle$. Higher in energy is a band of noninteracting intramonomer triplet-pair states.

Intermonomer triplet-pair states do not experience the strong intramonomer exchange interaction and consequently (neglecting for the moment the dipolar interaction to introduced shortly), the intermonomer triplet-pairs are noninteracting and space-separated. These pairs are labeled $^1|T \dots T\rangle$, $^3|T \dots T\rangle$ and $^5|T \dots T\rangle$ for the singlet, triplet and quintet states, respectively.

Triplets hop between adjacent ethylene dimers on neighboring lycopene monomers with a

transfer integral, $t_{\text{inter}} = 0.0088$ eV. This mechanism causes the intra and inter monomer singlet triplet-pairs to hybridize to form the lowest energy bimolecular singlet state,

$${}^1|\Psi\rangle = a|TT\rangle + b|T\cdots T\rangle. \quad (2)$$

As is shown in ref,²³ the mixing ratio a/b depends on the energy difference, Δ , between ${}^1|TT\rangle$ and ${}^1|T\cdots T\rangle$, with an exothermic process implying that $|b|^2 > |a|^2$. As also shown in ref,²³ a key emergent energy scale is ΔE_{QS} , the exchange energy between ${}^1|\Psi\rangle$ and the intermonomer quintet state, ${}^5|T\cdots T\rangle$. If $\Delta E_{QS} \ll k_B T$ full singlet fission occurs and the population of the initial ${}^1|TT\rangle$ becomes equally equilibrated between the singlet, triplet and quintet intermonomer pairs, implying free triplets on separate monomers. In this simulation the exothermic driving energy (defined in Fig. 2) is taken to be $\Delta = 0.44$ eV. This value is large enough to ensure that ΔE_{QS} is small enough such that singlet fission goes to completion at long times. It is also consistent with the energy level diagram shown in Fig. 3. Using this value of Δ , $\Delta E_{QS} = 1.16 \times 10^{-3}$ eV.

The final interaction to include in the triplet-pair Hamiltonian is the *intratriplet* dipolar (or zero-field-splitting) interaction. Assuming an axis of quantization along the principal dipolar axis, Z , this interaction reads³⁷

$$\hat{H}_{\text{ZFS}}^{\text{intra}} = \sum_{i=1}^2 D \left(\hat{S}_{iZ}^2 - \frac{1}{3} \hat{S}_i^2 \right) + \frac{E}{2} (\hat{S}_{i+}^2 + \hat{S}_{i-}^2), \quad (3)$$

where the sum is over both triplets in the pair, \hat{S} are again the spin-1 operators, and \hat{S}_{\pm} are the angular momentum shift operators. The first term couples the singlet triplet-pair with the $S_Z = 0$ component of the quintet triplet-pair, while the second term couples the singlet triplet-pair with the $S_Z = \pm 2$ components of the quintet triplet-pair. Since $D \sim 10^{-5}$ eV is already small compared to other energy scales and E is typically 10 to 100 times smaller than D ,^{36,37} the second term is neglected here.

In this work we take the intermonomer triplet transfer integral, t_{inter} , to be a parameter. In particular, the choice of $t_{\text{inter}}/t_{\text{intra}} = 0.01$ predicts a ${}^1|TT\rangle$ half-life of ca. 10 ps, which is consistent

with experimental observations.¹⁸ As shown in the SI, this choice implies a separation between the lycopene monomers in the H-aggregate of ca. 3 Å, which is consistent with the experimental absorption blue-shift of 0.92 eV.

We now turn to discuss the dynamical simulation. The triplet-pair dynamics are determined by the quantum Liouville equation, which is computed in the eigenstate basis of the two-monomer triplet-pair Hamiltonian.²³ Assuming the secular approximation, the quantum Liouville equation^{38,39} for the populations $P_a \equiv \rho_{aa}$ is,

$$\frac{dP_a}{dt} = - \sum_{b \neq a} (k_{ab}P_a - k_{ba}P_b) \quad (4)$$

while for the coherences it is,

$$\frac{d\rho_{ab}}{dt} = -i\omega_{ab}\rho_{ab} - 2\Gamma_{ab}(1 - \delta_{ab})\rho_{ab}. \quad (5)$$

The Bohr frequencies $\omega_{ab} = (E_a - E_b)/\hbar$, while $2\Gamma_{ab} = (\gamma_a + \gamma_b)$ and $\gamma_a = \sum_{b \neq a} k_{ab}$.

The inclusion of the ZFS interaction means that the energy eigenstates are not eigenstates of total spin. In this simulation we include both nonmagnetic and magnetic dephasing process. Thus, the thermal rates are a sum of the spin-conserving (SC) and spin-nonconserving (SNC) rates, i.e., $k_{ab} = (k_{ab}^{\text{SC}} + k_{ab}^{\text{SNC}})$, where k_{ab}^{SC} and k_{ab}^{SNC} are defined in the SI. Taking a reorganization energy of 0.05 eV,⁶ at 300 K the nonmagnetic dephasing time is calculated to be ca. 1 ps.²³ We take the characteristic time for the transverse (S_z -conserving magnetic) dephasing, T_2 , to be 10 ns. Assuming only transverse-spin dephasing and neglecting the spin-flip component of $\hat{H}_{\text{ZFS}}^{\text{intra}}$ means that only the $S_z = 0$ components of the triplet and quintet triplet-pairs states are connected to the singlet triplet-pairs states.

The triplet-pair basis and the two-monomer triplet-pair Hamiltonian are described in Section 2 of the SI; the parameters used in the simulation are listed in Section 3 of the SI. The solution of eqn (4) and eqn (5) is described in ref.²³

We now discuss the results of the dynamical simulation. Taking as our initial state $|\Psi\rangle =$

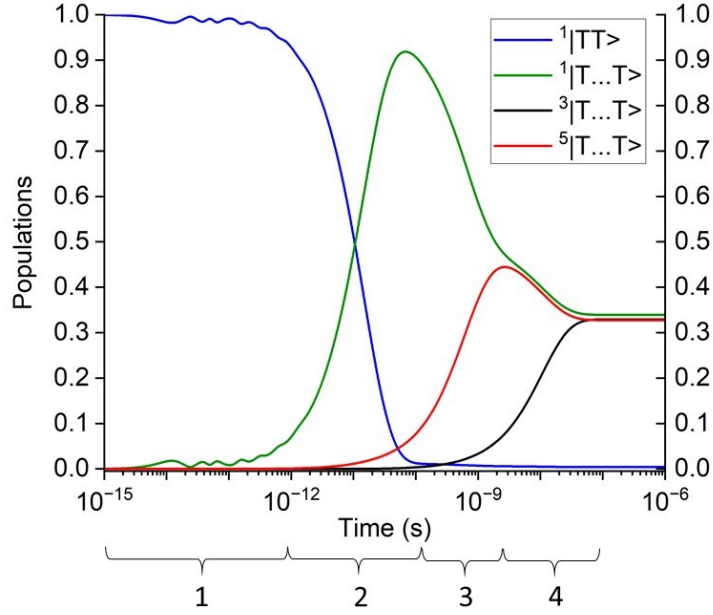


Figure 4: The populations as a function of time of the intramonomer singlet triplet-pair state, $^1|TT\rangle$, and the intermonomer singlet, triplet and quintet triplet-pair states, $^1|T\cdots T\rangle$, $^3|T\cdots T\rangle$ and $^5|T\cdots T\rangle$. The four time regimes are discussed in the text. This figure should be compared to Fig. 1.

$^1|TT\rangle \equiv |1^1B_u^-\rangle$, the triplet-pair populations are illustrated in Fig. 4. From this we can identify four time regimes:

1. Up to ca. 1 ps there is weak coherent dynamics between the intramonomer triplet pair, $^1|TT\rangle$, and the intermonomer triplet pair, $^1|T\cdots T\rangle$. As the system is off-resonance, the population is primarily $^1|TT\rangle$. This is represented as ‘1’ in the experimental transient excited state absorption¹⁸ shown in Fig. 1.
2. From ca. 1 ps to ca. 100 ps spin-conserving dephasing causes almost complete population transfer from $^1|TT\rangle$ to $^1|T\cdots T\rangle$. In so far as $^1|T\cdots T\rangle$ is a noninteracting triplet-pair, this is ‘singlet-fission’, although the system is still spin-correlated and the expectation value of $S^2 = 0$.
3. Next, from ca. 100 ps to ca. 2 ns the ZFS interaction mixes the singlet and quintet intermonomer triplet-pair states. Since this process is over damped, there are no oscillations.

Moreover, as $D/\Delta E_{QS} \simeq 0.01$, the population ratio of $^1|T \cdots T\rangle$ to $^5|T \cdots T\rangle$ does not equal 1:2, as it would do if $D/\Delta E_{QS} \gg 1$. As $^1|T \cdots T\rangle$ and $^5|T \cdots T\rangle$ are spectroscopically indistinguishable, the time regimes 2 and 3 are represented as ‘2’ in Fig. 1.

4. Finally, after ca. 2 ns and within ca. 100 ns transverse spin-dephasing equilibrates $^1|T \cdots T\rangle$, $^3|T \cdots T\rangle$ and $^5|T \cdots T\rangle$ to a population of 1/3 each. Equivalently, this population corresponds to spin-uncorrelated, single triplets^{23,40} on separate monomers and is represented by ‘3’ in Fig. 1.

In summary, the proposed mechanism of singlet fission in lycopene H-aggregates is the following. Optical excitation of the aggregate excites a high-energy bright state (S_n) that is partially delocalized over the aggregate. This state rapidly relaxes and localizes onto a single lycopene monomer, populating an intermediate, singlet triplet-pair state. This is the $1^1B_u^-$ state, often labeled S_1^* . As explained in this letter, this state is the second member of the strongly correlated ‘ $2A_g$ ’ family of states. It is the strongly bound, intramonomer triplet-pair state, also labeled $^1|TT\rangle$, whose population dynamics are illustrated in Fig. 4. Internal conversion from the $1^1B_u^-$ state to the $2^1A_g^-$ state is assumed to be slow, because it is symmetry forbidden. Next, the $1^1B_u^-$ state undergoes ‘fission’ into noninteracting, spin-correlated triplet pairs on separate monomers, labeled $^1|T \cdots T\rangle$. Because fission from the $1^1B_u^-$ state is quite exothermic, within ca. 100 ps there is almost complete population transfer from $^1|TT\rangle$ to $^1|T \cdots T\rangle$. Following the population of $^1|T \cdots T\rangle$, the ZFS interaction mixes $^1|T \cdots T\rangle$ and $^5|T \cdots T\rangle$. Finally, hyperfine interactions mix $^1|T \cdots T\rangle$, $^3|T \cdots T\rangle$ and $^5|T \cdots T\rangle$. Since $\Delta E_{QS}/k_B T \simeq 0.04$ (and we only consider transverse dephasing), the populations are equal. This final mixed state corresponds to spin-uncorrelated, single triplets on separate monomers,^{23,40} i.e., $|T_1\rangle + |T_1\rangle$.

This letter has focussed on singlet fission in lycopene H-aggregates. However, other carotenoid H-aggregates also exhibit singlet fission with photophysical behavior semiquantitatively similar to that described here. For example, Quaranta and co-workers¹⁹ investigated singlet fission in lutein and violaxanthin H-aggregates. In common with lycopene, these carotenoids possess C_2 symmetry. Following photoexcitation of the aggregate, Quaranta and co-workers¹⁹ propose an intermediate

state that participates in singlet fission, which they nominated as a vibrationally hot S_1 state. In light of the work described here, however, we think that this state is more likely to be a distinct (albeit a related) electronic state, namely the $1^1B_u^-$ state.

In conclusion, this letter describes a theory of singlet fission in lycopene H-aggregates that is in semiquantitative agreement with experimental observations.¹⁸ In particular, the theory assumes that singlet fission in carotenoid systems occurs via an intermediate, intramonomer singlet triplet-pair state (i.e., $1^1B_u^-$), which facilitates exothermic intermonomer singlet fission. This state is populated via the excitation of a higher energy H-aggregate bright state. In contrast, singlet fission in polyacenes occurs directly from the intramolecular bright state. Thus, the participation of an intramolecular triplet-pair state in carotenoid singlet fission implies that this mechanism is quite different from that of polyacenes.

Supporting Information

1. The Hubbard-UV-Peierls Hamiltonian

The DMRG calculations^{31,33} of the electronic states of lycopene were performed using the Hubbard-UV-Peierls Hamiltonian. This Hamiltonian has three components.

The purely electronic Hubbard-UV Hamiltonian is

$$\hat{H}_{\text{UV}} = -2 \sum_{n=1}^{N-1} \beta_n \hat{T}_n + U \sum_{n=1}^N (\hat{N}_{n\uparrow} - \frac{1}{2})(\hat{N}_{n\downarrow} - \frac{1}{2}) + \frac{1}{2} \sum_{n=1}^{N-1} V (\hat{N}_n - 1)(\hat{N}_{n+1} - 1), \quad (6)$$

which contains a nearest neighbor electron transfer term, β_n , and onsite and nearest neighbor Coulomb interactions, U and V , respectively. $\hat{T}_n = \frac{1}{2} \sum_{\sigma} (c_{n,\sigma}^{\dagger} c_{n+1,\sigma} + c_{n+1,\sigma}^{\dagger} c_{n,\sigma})$ is the bond order operator, \hat{N}_n is the number operator and N ($= 22$ for lycopene) is the number of conjugated carbon-atoms ($N/2$ is the number of double bonds).

The electrons couple to the nuclei via changes in the C-C bond length (which changes the effective electron transfer integral)

$$\hat{H}_{\text{e-n}} = 2\alpha \sum_{n=1}^{N-1} (u_{n+1} - u_n) \hat{T}_n, \quad (7)$$

where α is the electron-nuclear coupling parameter and u_n is the displacement of nucleus n from its undistorted position.

Finally, the nuclear potential energy is described by

$$\hat{H}_{\text{elastic}} = \frac{K}{2} \sum_{n=1}^{N-1} (u_{n+1} - u_n)^2, \quad (8)$$

where K is the nuclear spring constant.

The Hubbard-UV-Peierls Hamiltonian is defined as

$$\hat{H}_{\text{UVP}} = \hat{H}_{\text{UV}} + \hat{H}_{\text{e-n}} + \hat{H}_{\text{elastic}}. \quad (9)$$

This Hamiltonian is invariant under both a two-fold proper rotation (i.e., a C_2 operation) and a particle-hole transformation (i.e., $(\hat{N} - 1) \rightarrow -(\hat{N} - 1)$), and so its eigenstates are labeled either A_g^\pm or B_u^\pm .

The parameters are the same as used in previous work,^{22,30} i.e., $\beta = 2.4$ eV, $U = 7.25$ eV, $K = 46$ eV⁻² and $\alpha = 4.6$ eV⁻¹. As described in the main paper, in order to model relative $2^1A_g^-/1^1B_u^+$ energies we make two choices for V , i.e., $V = 2.75$ eV or $V = 3.25$ eV.

2. The Triplet-Pair Basis and Hamiltonian

The initial singlet triplet-pair state, $^1|TT\rangle$, is²⁸

$$^1|TT\rangle = \sum_{ij \in \times = 1} \Phi_{ij} ^1|i, j\rangle, \quad (10)$$

where the singlet triplet-pair basis state is

$$^1|i, j\rangle = \frac{1}{\sqrt{3}} (|1; i\rangle|-1; j\rangle - |0; i\rangle|0; j\rangle + |-1; i\rangle|1; j\rangle), \quad (11)$$

$|S_Z; i\rangle$ is a triplet on ethylene dimer i with spin projection S_Z , Φ_{ij} is the lowest eigenstate of the one-monomer Hamiltonian (defined below) with B_u symmetry, and $ij \in \times = 1$ in eqn (10) implies that dimers i and j are on monomer 1.

As described in the main paper, triplets on the same monomer experience the exchange interaction,^{23,36}

$$\hat{H}_{\text{exchange}} = J \hat{\mathbf{S}}_i \cdot \hat{\mathbf{S}}_{i+1}, \quad (12)$$

where $\hat{\mathbf{S}}$ is the spin-1 (triplet) operator and J is the *inter*triplet exchange interaction.

Triplets also experience the *intra*triplet dipolar (or zero-field-splitting) interaction,

$$\hat{H}_{\text{ZFS}}^{\text{intra}} = \sum_{i=1}^2 D \left(\hat{S}_{iZ}^2 - \frac{1}{3} \hat{S}_i^2 \right), \quad (13)$$

where the only the S_z conserving component is retained.

In this work we investigate the role of transverse spin-dephasing and the component of the ZFS-Hamiltonian which connects the $S_z = 0$ components of each total spin. The $S_z = 0$ components of the triplet and quintet triplet-pair bases are,

$${}^3|i, j\rangle = \frac{1}{\sqrt{2}} (|1; i\rangle| - 1; j\rangle - | - 1; i\rangle|1; j\rangle), \quad (14)$$

and

$${}^5|i, j\rangle = \frac{1}{\sqrt{6}} (|1; i\rangle| - 1; j\rangle + 2|0; i\rangle|0; j\rangle + | - 1; i\rangle|1; j\rangle), \quad (15)$$

respectively.

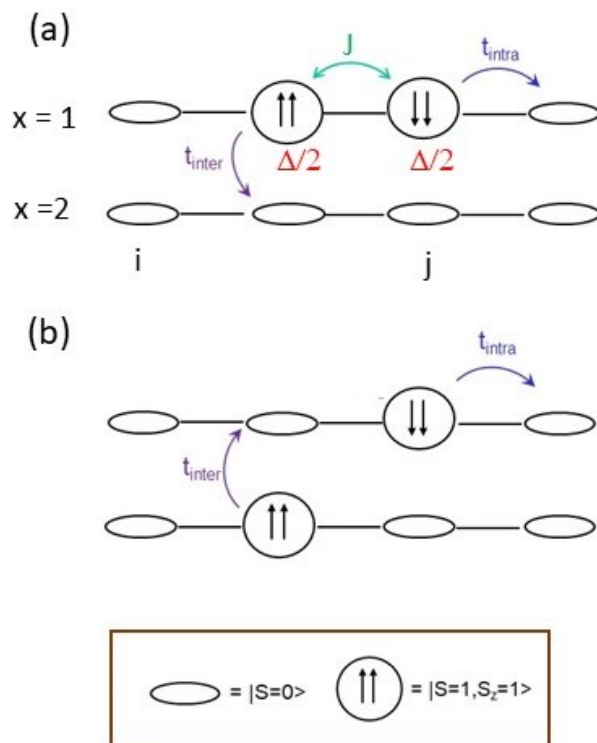


Figure 5: A schematic illustration of a carotenoid dimer. (a) with a triplet-pair on monomer $x = 1$, with triplets on ethylene dimers i and j . Monomer $x = 2$ is in its ground state. This represents $\hat{H}_{\text{exchange}} + \hat{H}_{\text{single}}^{\times=1,2}$. (b) represents $\hat{H}_{\text{double}} + \hat{H}_{\text{inter}}$. t_{intra} and t_{inter} are the hopping matrix elements between neighboring intramonomer and intermonomer ethylene dimers, respectively.

The triplets hop between neighboring dimers on the same monomer (see Fig. 5(a)), described by

$$\hat{H}_{\text{single}}^{\times=1,2} = \Delta \sum_{i,j>i \in \times} |i,j\rangle\langle i,j| + t_{\text{intra}} \sum_{i \neq j \in \times} (|i \pm 1, j\rangle\langle i, j| + \text{H.C.}), \quad (16)$$

Δ is the exothermic driving energy of $1^1B_u^-$ relative to two single triplets on separate monomers. Triplets on separate monomers hop between neighboring dimers on the same monomer (see Fig. 5(b)), described by

$$\hat{H}_{\text{double}} = t_{\text{intra}} \sum_{i \in \times=1} \sum_{j \in \times=2} [(|i \pm 1, j\rangle\langle i, j| + \text{H.C.}) + (|i, j \pm 1\rangle\langle i, j| + \text{H.C.})], \quad (17)$$

and between adjacent dimers on neighboring monomers (see Fig. 5(b)), described by

$$\hat{H}_{\text{inter}} = t_{\text{inter}} \sum_{\times=1}^2 \sum_{i_{\times}} \sum_{j_{\times}>i_{\times}} [(|i_{\times}, j_{\times}\rangle\langle i_{\bar{\times}}, j_{\bar{\times}}| + \text{H.C.}) + (|i_{\times}, j_{\times}\rangle\langle i_{\times}, j_{\bar{\times}}| + \text{H.C.})]. \quad (18)$$

3. Model Parameters

Table 1 lists the parameters used in the two-monomer triplet-pair Hamiltonian described in Section 2, as well as the parameters used in the quantum Liouville equation.

Table 1: Values of input and derived parameters.

Parameter	Value
Intramonomer triplet exchange interaction, ²³ J	1.23 eV
Intramonomer triplet transfer integral, ²⁸ t_{intra}	0.88 eV
Intermonomer triplet transfer integral, t_{inter}	0.0088 eV
Exothermic driving energy, Δ	0.44 eV
Intratriplet dipolar interaction, D	10^{-5} eV
Reorganization energy, λ	0.05 eV
Spectral function cut-off frequency, ω_0	0.2 eV
Temperature	300 K
Spin-dephasing factor, γ	10^{-4}
Derived two-monomer quintet-singlet exchange energy, ΔE_{QS}	1.16×10^{-3} eV

4. Computation of Interstate Rates

The inclusion of the ZFS interaction into the two-monomer triplet-pair Hamiltonian means that the energy eigenstates are not eigenstates of total spin. In the simulation we include both nonmagnetic and magnetic dephasing processes. To account for this the thermal rates that appear in quantum Liouville equation are defined as the sum of the spin-conserving (SC) and spin-nonconserving (SNC) rates, i.e.,

$$k_{ab} = k_{ab}^{\text{SC}} + k_{ab}^{\text{SNC}}. \quad (19)$$

Defining the Bohr frequencies as $\omega_{ab} = (E_a - E_b)/\hbar$ and taking $\omega_{ab} \geq 0$, the spin-conserving thermal rates are,^{38,39}

$$k_{ab}^{\text{SC}} = \left(\frac{2\lambda}{\hbar} \right) J(\omega_{ab}) (n(\omega_{ab}) + 1) C_{ab}^{\text{SC}} \quad (20)$$

and

$$k_{ba}^{\text{SC}} = \left(\frac{2\lambda}{\hbar} \right) J(\omega_{ab}) n(\omega_{ab}) C_{ab}^{\text{SC}}, \quad (21)$$

where $n(\omega) = (\exp\beta\hbar\omega - 1)^{-1}$ is the Bose distribution function, $J(\omega) = \omega\omega_0/(\omega^2 + \omega_0^2)$ is the (dimensionless) Debye-spectral function, ω_0 is the cut-off frequency and λ is the bath reorganization energy. The parameters are listed in Table 1.

The spin-conserving overlap factors are,

$$C_{ab}^{\text{SC}} = 2 \sum_m S_{ma}^2 S_{mb}^2. \quad (22)$$

Here, a and b label energy eigenstates of the two-monomer Hamiltonian, whereas m labels a real-space basis state of the triplet-pair states.²³ In particular, m encodes the dimer locations of each triplet in the pair, as well as the total spin of the pair. \mathbf{S} is the matrix whose columns are the eigenvectors of the two-monomer Hamiltonian represented in the real-space basis. Thus, $S_{ma}^2 = P_{ma}$ is the probability that the a th energy eigenstate occupies the m th real-space basis state.

Similarly, the spin-nonconserving thermal rates are,

$$k_{ab}^{\text{SNC}} = \gamma \left(\frac{2\lambda}{\hbar} \right) J(\omega_{ab}) (n(\omega_{ab}) + 1) C_{ab}^{\text{SNC}} \quad (23)$$

and

$$k_{ba}^{\text{SNC}} = \gamma \left(\frac{2\lambda}{\hbar} \right) J(\omega_{ab}) n(\omega_{ab}) C_{ab}^{\text{SNC}}, \quad (24)$$

where γ is a factor to take into account weaker transverse spin-dephasing than spin-conserving dephasing. We take $\gamma = 10^{-4}$, which at 300 K implies $T_2 \sim 10$ ns.

The spin-nonconserving overlap factors are,

$$C_{ab}^{\text{SNC}} = \sum_m f_{m\bar{m}} (S_{ma}^2 S_{\bar{m}b}^2 + S_{\bar{m}a}^2 S_{mb}^2), \quad (25)$$

where the label \bar{m} refers to the same triplet-pair dimers as m , but corresponds to a different spin-eigenstate, i.e., singlet, triplet or quintet. In addition, $f_{m\bar{m}} = 2/3$ for singlet-triplet transitions, $f_{m\bar{m}} = 1/3$ for triplet-quintet transitions, and $f_{m\bar{m}} = 0$ for singlet-quintet transitions.²³

5. Intermonomer Triplet-Pair Coupling

The simulations of singlet fission in this work took the intermonomer triplet transfer integral, t_{inter} , to be a parameter. In particular, the choice of $t_{\text{inter}}/t_{\text{intra}} = 0.01$ results in a half-life of the intra-monomer singlet triplet-pair, $^1|TT\rangle$, to be ca. 10 ps. This value is consistent with the experimental observations of Kundu and Dasgupta¹⁸ (see Fig. 1). Indeed, the $^1|TT\rangle$ half-life is rather sensitive to $t_{\text{inter}}/t_{\text{intra}}$: values of $t_{\text{inter}}/t_{\text{intra}} = 0.01$, 0.001 and 0.0001 predict half-lives of 10 ps, 1 ns and 100 ns, respectively.

As explained in ref.²³ both intra and inter monomer triplet transfer is assumed to be a superexchange process, mediated by a virtual charge-transfer exciton. Thus, $t \propto \beta^2$, where β is the p_z -orbital resonance integral. We therefore deduce that $\beta_{\text{inter}}/\beta_{\text{intra}} = 0.1$. Using the Mulliken

expression⁴¹ for β , i.e.,

$$\beta = (10.6 \text{ eV}) \times \exp(-r\xi) \left(1 + r\xi + \frac{2}{5}(r\xi)^2 + \frac{1}{15}(r\xi)^3 \right), \quad (26)$$

where r is in \AA and $\xi = 3.07 \text{ \AA}^{-1}$, we can now estimate the intermolecular separation. Taking the single bond length $r_{\text{single}} = 1.45 \text{ \AA}$ implies that $\beta_{\text{intra}} = 2.4 \text{ eV}$ and thus $\beta_{\text{inter}} = 0.24 \text{ eV}$. Again, using eqn (26), we find that the intermonomer separation is thus predicted to be 2.9 \AA .

As we now show, a separation of ca. 3 \AA between the lycopene monomers in the H-aggregate is consistent with a blue shift of 0.92 eV , as measured in ref.¹⁸ According to the line-dipole theory of exciton transfer integrals,⁴² the exciton transfer integral, J , between two conjugated molecules of length L and separation r is

$$J = \left(\frac{\mu^2}{4\pi\epsilon_0 r^3} \right) \left(\frac{2}{(L/r)^2} \right) \left(1 - \frac{1}{\sqrt{1 + (L/r)^2}} \right), \quad (27)$$

where μ is the transition dipole moment.

According to DMRG calculations,³³ $\mu = 5.71 \times 10^{-29} \text{ Cm}$ for a lycopene monomer of 22 conjugated C-atoms. The measured blue-shift in a H-aggregate is approximately zJ , where z is the number of nearest neighbors to which each monomer is dipole coupled. Using $zJ = 0.92 \text{ eV}$ and $r = 2.9 \text{ \AA}$, we find that $z = 4.6$. This result seems very reasonable and places confidence that, as well as being empirically justified, our parameter choice of $t_{\text{inter}}/t_{\text{intra}} = 0.01$ is physically realistic.

References

- (1) Smith, M. B.; Michl, J. Singlet Fission. *Chemical Reviews* **2010**, *110*, 6891–6936.
- (2) Casanova, D. Theoretical Modeling of Singlet Fission. *Chemical Reviews* **2018**, *118*, 7164–7207.
- (3) Musser, A. J.; Clark, J. Triplet-Pair States in Organic Semiconductors. *Annual Review of Physical Chemistry* **2019**, *70*, 323.
- (4) Sanders, S. N.; Pun, A. B.; Parenti, K. R.; Kumarasamy, E.; Yablon, L. M.; Sfeir, M. Y.; Compos, L. M. Understanding the Bound Triplet-Pair State in Singlet Fission. *Chem* **2019**, *5*, 1988.
- (5) Miyata, K.; Conrad-Burton, F. S.; Geyer, F. L.; Zhu, X. Y. Triplet Pair States in Singlet Fission. *Chemical Reviews* **2019**, *119*, 4261–4292.
- (6) Berkelbach, T. C.; Hybertsen, M. S.; Reichman, D. R. Microscopic theory of singlet exciton fission. II. Application to pentacene dimers and the role of superexchange. *Journal of Chemical Physics* **2013**, *138*.
- (7) Aryanpour, K.; Shukla, A.; Mazumdar, S. Theory of Singlet Fission in Polyenes, Acene Crystals, and Covalently Linked Acene Dimers. *Journal of Physical Chemistry C* **2015**, *119*, 6966–6979.
- (8) Fallon, K. J.; Sawhney, N.; Toolan, D. T. W.; Sharma, A.; Zeng, W. X.; Montanaro, S.; Leventis, A.; Dowland, S.; Millington, O.; Congrave, D.; Bond, A.; Friend, R.; Rao, A.; Bronstein, H. Quantitative Singlet Fission in Solution-Processable Dithienohexatrienes. *Journal of the American Chemical Society* **2022**, *144*, 23516–23521.
- (9) Millington, O.; Montanaro, S.; Leventis, A.; Sharma, A.; Dowland, S. A.; Sawhney, N.; Fallon, K. J.; Zeng, W. X.; Congrave, D. G.; Musser, A. J.; Rao, A. K.; Bronstein, H. Solu-

- ble Diphenylhexatriene Dimers for Intramolecular Singlet Fission with High Triplet Energy. *Journal of the American Chemical Society* **2023**, *145*, 2499–2510.
- (10) Kraabel, B.; Hulin, D.; Aslangul, C.; Lapersonne-Meyer, C.; Schott, M. Triplet exciton generation, transport and relaxation in isolated polydiacetylene chains: subpicosecond pump-probe experiments. *Chemical Physics* **1998**, *227*, 83.
- (11) Lanzani, G.; Stagira, S.; Cerullo, G.; De Silvestri, S.; Comoretto, D.; Moggio, I.; Cuniberti, C.; Musso, G. F.; Dellepiane, G. Triplet exciton generation and decay in a red polydiacetylene studied by femtosecond spectroscopy. *Chemical Physics Letters* **1999**, *313*, 525.
- (12) Musser, A. J.; Al-Hashimi, M.; Maiuri, M.; Brida, D.; Heeney, M.; Cerullo, G.; Friend, R. H.; Clark, J. Activated Singlet Exciton Fission in a Semiconducting Polymer. *Journal of the American Chemical Society* **2013**, *135*, 12747.
- (13) Wang, C.; Tauber, M. J. High-Yield Singlet Fission in a Zeaxanthin Aggregate Observed by Picosecond Resonance Raman Spectroscopy. *Journal of the American Chemical Society* **2010**, *132*, 13988–13991.
- (14) Wang, C.; Schlamadinger, D. E.; Desai, V.; Tauber, M. J. Triplet Excitons of Carotenoids Formed by Singlet Fission in a Membrane. *Chemphyschem* **2011**, *12*, 2891–2894.
- (15) Trinh, M. T.; Zhong, Y.; Chen, Q. S.; Schiros, T.; Jockusch, S.; Sfeir, M. Y.; Steigerwald, M.; Nuckolls, C.; Zhu, X. Y. Intra- to Intermolecular Singlet Fission. *Journal of Physical Chemistry C* **2015**, *119*, 1312–1319.
- (16) Musser, A. J.; Maiuri, M.; Brida, D.; Cerullo, G.; Friend, R. H.; Clark, J. The Nature of Singlet Exciton Fission in Carotenoid Aggregates. *Journal of the American Chemical Society* **2015**, *137*, 5130.
- (17) Llansola-Portoles, M. J.; Redeckas, K.; Streckaite, S.; Iljoaia, C.; Pascal, A. A.; Telfer, A.;

- Vengris, M.; Valkunas, L.; Robert, B. Lycopene crystalloids exhibit singlet exciton fission in tomatoes. *Physical Chemistry Chemical Physics* **2018**, *20*, 8640–8646.
- (18) Kundu, A.; Dasgupta, J. Photogeneration of Long-Lived Triplet States through Singlet Fission in Lycopene H-Aggregates. *Journal of Physical Chemistry Letters* **2021**, *12*, 1468–1474.
- (19) Quaranta, A.; Krieger-Liszkay, A.; Pascal, A. A.; Perreau, F.; Robert, B.; Vengris, M.; Llansola-Portoles, M. J. Singlet fission in naturally-organized carotenoid molecules. *Physical Chemistry Chemical Physics* **2021**, *23*, 4768–4776.
- (20) Kim, H.; Zimmerman, P. M. Coupled double triplet state in singlet fission. *Physical Chemistry Chemical Physics* **2018**, *20*, 30083–30094.
- (21) Santra, S.; Ray, J.; Ghosh, D. Mechanism of Singlet Fission in Carotenoids from a Polyene Model System. *Journal of Physical Chemistry Letters* **2022**, *13*, 6800–6805.
- (22) Manawadu, D.; Georges, T. N.; Barford, W. Photoexcited State Dynamics and Singlet Fission in Carotenoids. *Journal of Physical Chemistry A* **2023**, *127*, 1342.
- (23) Barford, W.; Chambers, C. A. Theory of Singlet Fission in Carotenoid Dimers. *Journal of Chemical Physics* **2023**, *159*, 084116.
- (24) Gradinaru, C. C.; Kennis, J. T. M.; Papagiannakis, E.; van Stokkum, I. H. M.; Cogdell, R. J.; Fleming, G. R.; Niederman, R. A.; van Grondelle, R. An unusual pathway of excitation energy deactivation in carotenoids: Singlet-to-triplet conversion on an ultrafast timescale in a photosynthetic antenna. *Proceedings of the National Academy of Sciences of the United States of America* **2001**, *98*, 2364–2369.
- (25) Rondonuwu, F. S.; Watanabe, Y.; Fujii, R.; Koyama, Y. A first detection of singlet to triplet conversion from the $1^1B_u^+$ to the 1^1A_g state and triplet internal conversion from the 1^1A_g to the 1^3B_u state in carotenoids: dependence on the conjugation length. *Chemical Physics Letters* **2003**, *376*, 292–301.

- (26) Hudson, B. S.; Kohler, B. E. Low-Lying Weak Transition in Polyene Alpha, Omega-Diphenyloctatetraene. *Chemical Physics Letters* **1972**, *14*, 299.
- (27) Schulten, K.; Karplus, M. Origin of a Low-Lying Forbidden Transition in Polyenes and Related Molecules. *Chemical Physics Letters* **1972**, *14*, 305.
- (28) Barford, W. Theory of the Dark State of Polyenes and Carotenoids. *Phys. Rev. B* **2022**, *106*, 35201.
- (29) Valentine, D. J.; Manawadu, D.; Barford, W. Higher-energy triplet-pair states in polyenes and their role in intramolecular singlet fission. *Physical Review B* **2020**, *102*, 125107.
- (30) Manawadu, D.; Valentine, D. J.; Marcus, M.; Barford, W. Singlet Triplet-Pair Production and Possible Singlet-Fission in Carotenoids. *Journal of Physical Chemistry Letters* **2022**, *13*, 1344.
- (31) Manawadu, D.; Valentine, D. T.; Barford, W. Dynamical simulations of carotenoid photoexcited states using density matrix renormalization group techniques. *Journal of Physical Chemistry A* **2023**, *127*, 3714.
- (32) Mannouch, J. R.; Barford, W.; Al-Assam, S. Ultra-fast relaxation, decoherence, and localization of photoexcited states in pi-conjugated polymers. *J Chem Phys* **2018**, *148*, 034901.
- (33) Barford, W.; Bursill, R. J.; Lavrentiev, M. Y. Density-matrix renormalization-group calculations of excited states of linear polyenes. *Physical Review B* **2001**, *63*, 195108.
- (34) Taffet, E. J.; Lee, B. G.; Toa, Z. S. D.; Pace, N.; Rumbles, G.; Southall, J.; Cogdell, R. J.; Scholes, G. D. Carotenoid Nuclear Reorganization and Interplay of Bright and Dark Excited States. *Journal of Physical Chemistry B* **2019**, *123*, 8628.
- (35) Khokhlov, D.; Belov, A. Ab Initio Study of Low-Lying Excited States of Carotenoid-Derived Polyenes. *Journal of Physical Chemistry A* **2020**, *124*, 5790.

- (36) Kollmar, C. Electronic-Structure of Diradical and Dicarbene Intermediates in Short-Chain Polydiacetylene Oligomers. *Journal of Chemical Physics* **1993**, *98*, 7210–7228.
- (37) Weil, J. A.; Bolton, J. R. *Electron paramagnetic resonance : elementary theory and practical applications*, 2nd ed.; Wiley ; Chichester : John Wiley: Hoboken, N.J., 2007.
- (38) Nitzan, A. *Chemical dynamics in condensed phases : relaxation, transfer and reactions in condensed molecular systems*; Oxford graduate texts; Oxford University Press: Oxford, 2006.
- (39) May, V.; Kühn, O. *Charge and energy transfer dynamics in molecular systems*; Wiley-VCH: Weinheim, 2011.
- (40) Scholes, G. D. Correlated Pair States Formed by Singlet Fission and Exciton-Exciton Annihilation. *Journal of Physical Chemistry A* **2015**, *119*, 12699–12705.
- (41) Mulliken, R. S.; Rieke, C. A.; Orloff, D.; Orloff, H. Overlap Integrals and Chemical Binding. *Journal of Chemical Physics* **1949**, *17*, 510.
- (42) Barford, W. Exciton transfer integrals between polymer chains. *Journal of Chemical Physics* **2007**, *126*, 134905.